PHYSICAL REVIEW B **79**, 020201(R) (2009)

Universal acoustic dispersion in liquid alkali metals

Valentina M. Giordano and Giulio Monaco
European Synchrotron Radiation Facility, 6 rue Jules Horowitz, B.P. 440, 38043 Grenoble CEDEX, France
(Received 1 October 2008; published 7 January 2009)

The high-frequency acoustic dynamics of liquid cesium has been investigated by inelastic x-ray scattering as a function of pressure up to 5 GPa, corresponding to a volume compression of 50%. The obtained acoustic dispersion curves are found to scale on a single master curve, which turns out to be followed also by all the data available in the literature for liquid alkali metals, spanning a very large density range. This shows that the high-frequency acoustic modes of these systems are largely unaffected by the details of the relaxation dynamics characteristic of the macroscopic limit. Moreover, we find that a common model of interatomic potential describes them with good approximation for very different packing fractions and electronic screening contributions.

DOI: 10.1103/PhysRevB.79.020201 PACS number(s): 61.05.cf, 61.25.Mv, 62.50.−p, 63.50.−x

The understanding of the microscopic dynamics in liquids and especially of its relation to the interparticle potential is a long-standing issue.[1] A great number of theoretical and experimental studies have been devoted to it over the years, mostly focusing on simple liquids with isotropic pair interaction, such as rare gases and alkali metals. The latter ones in particular have been constantly addressed as they also allow for the study of the electron screening on the ion-ion interaction in nearly free-electron systems. For example, all alkali metals have been investigated at their melting point either by inelastic neutron (INS) (Refs. 2–4) or x-ray scattering (IXS),[5–7] two techniques that probe density fluctuations. These experiments have revealed (i) the existence of well-defined long-living collective excitations propagating up to wave vectors q well beyond the region of validity of simple hydrodynamics and (ii) a marked enhancement of the sound velocity over the hydrodynamic limit (positive dispersion). These common features and the existence of scaling laws for a number of physical properties[8] have stimulated a theoretical effort toward a unitary description of liquid alkali metals. In particular, Balucani *et al.*[9,10] found that the model of potential developed by Price *et al.*[11] could reproduce the structural and dynamical properties observed in liquid Na, K, Rb, and Cs at their melting point and could assume a universal form in properly reduced units. Specifically, they found that (i) the static structure factor scales in the reduced exchanged momentum $\tilde{q}=q\sigma$, σ being the position of the first zero of the potential, and that (ii) the same holds true for the acoustic dispersion curves $\Omega(q)$ in the normalized units $\tilde{q}$ and $\tilde{\Omega}=\Omega(q)\tau_B$, where $\tau_B=\sqrt{M\sigma^2/\epsilon}$ sets the typical timescale in Lennard-Jones liquids, ϵ being the potential-well depth and M the ionic mass.[9,10]

So far, the experimental investigation of the high-frequency dynamics of liquid alkali metals has been mostly limited to thermodynamic conditions very close to the melting point, where they are characterized by a very similar packing fraction $\eta=\pi n\sigma^3/6$ (n being the number density), and only few studies were performed at high temperature.[12–14] Among them, the study of liquid Rb by Pilgrim and Morkel[8] reports that in a large temperature range the acoustic dispersion curves are basically the same as those at melting, indicating an unchanged interparticle interaction, while at low-enough density drastic changes in the dynamics were ascribed to an occurring dimerization. No experimental data are instead available on the opposite limit, i.e., at high densities; this limit is, however, of utmost interest as it allows for the tuning of the interplay between the electronic screening and the bare ion-ion interaction. Indeed, at high density on one hand the electronic screening increases and on the other hand the effect of the ion core size becomes more relevant as the interparticle distance is reduced.

Among the alkali metals, Cs is the most favorable system for a high-pressure investigation due to its high compressibility which allows for the observation already below 10 GPa of phase transitions and changes in the electronic band structure, which in other alkali metals are only observed at higher pressure. For example, a first-order structural transition was recently reported in liquid Cs at ≈3.8 GPa, driven by a pressure-induced *s-d* hybridization similar to the one reported in the solid phase at ≈4.3 GPa.[15,16] For this reason, we have performed an IXS investigation of the high-frequency dynamics of liquid Cs at high pressure, up to a volume contraction of 50%. We show in the following that the measured acoustic excitations scale on a single universal dispersion curve which is actually also followed by all the other existing data for liquid alkali metals. This clearly suggests that a single model of interatomic potential is able to describe the dynamical properties of this class of systems with good approximation.

The IXS experiment was carried out on the ID16 beamline at the ESRF,[17] using an incident energy of 17 793 eV and an energy resolution of 3 meV [full width at half maximum (FWHM)]. The spectra were collected in the exchanged energy range of [−20–20] meV and in the q range of [1.5–28] nm^{-1}, with a total integration time of 450 s/point. High-purity Cs powder was loaded in a membrane diamond-anvil cell (DAC) in Ar atmosphere. A Re gasket was used as it is known not to react with the high-temperature liquid.[15] An external resistive heater allowed us to keep a constant temperature at $T=493$ K, measured by a thermocouple cemented to one of the diamonds. Five pressure points were investigated between 0.3 and 5 GPa, just up to the solidification point. The pressure was derived from the position q_0 of the main peak of the structure factor, $S(q)$, which had been previously calibrated against the equation of

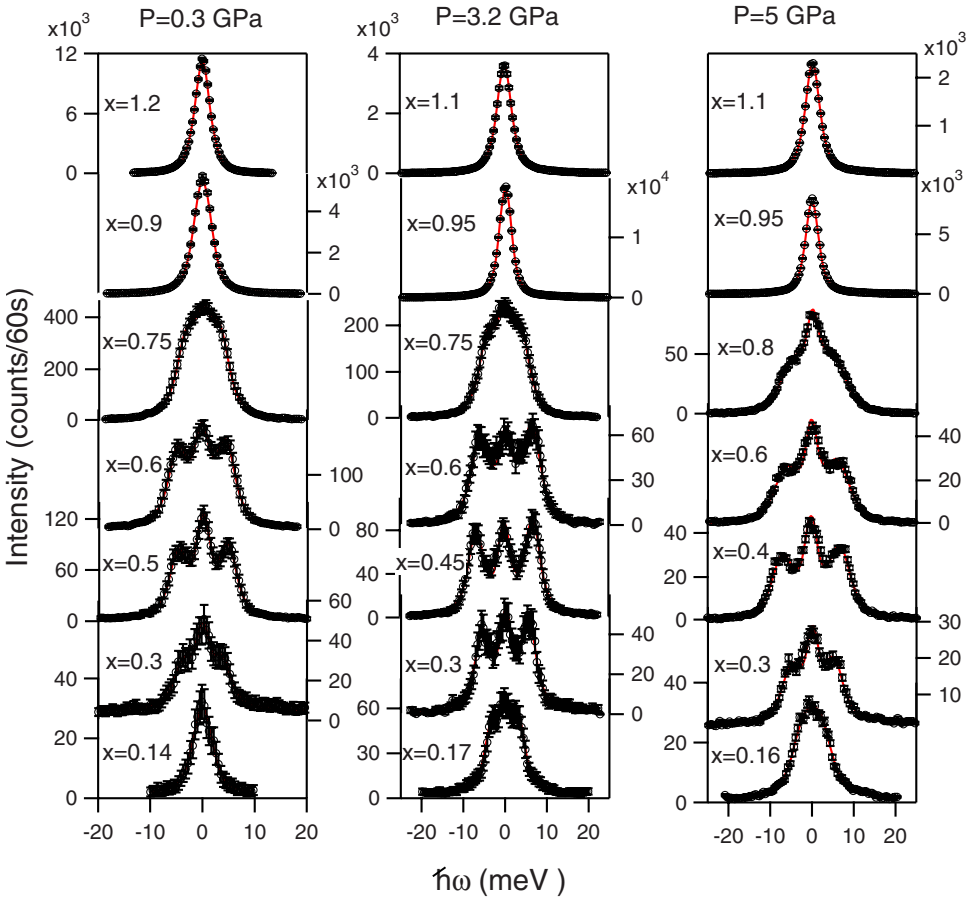

FIG. 1. (Color online) Selected IXS spectra of Cs collected at $T=493$ K and $P=0.3$, 3.2, and 5 GPa are reported together with the model used to describe them (red solid lines). The spectra are shown at similar values of $x=q/q_0$ to highlight the differences, where $q_0=14.67$, 17.5, and 18.6 nm^{-1}, respectively.

state of molybdenum[18] in a dedicated x-ray diffraction experiment performed on the ID09 beamline at the ESRF. These $S(q)$ data have been analyzed in order to extract the pair-correlation function $g(r)$ and will be presented elsewhere.

A selection of spectra collected at different pressures is reported in Fig. 1. These spectra are directly proportional to the dynamic structure factor $S(q,\omega)$ after convolution to the instrumental function. It is known that for liquid alkali metals the $S(q,\omega)$ can be well described in the framework of generalized hydrodynamics, taking into account the presence of one or two relaxation processes.[1] In the present case, however, a good description of the spectra could be given (see Fig. 1) by the simpler model based on a delta function for the elastic line and a damped harmonic-oscillator function for the inelastic features.[19] Our results for the position of the inelastic excitations, corresponding to the parameter Ω of this model, are reported in Fig. 2 together with those for the apparent phase velocity $v=\Omega/q$. The data corresponding to the three selected pressure points are qualitatively similar. The application of pressure results, on one hand, in an increase in the acoustic frequencies and in the sound velocity, and—on the other hand—in a widening of the q scale due to the expansion of the pseudo-Brillouin zone. The dispersion curve and the velocity measured by INS at the room pressure melting point (308 K) (Ref. 3) are also shown for comparison (dashed lines in Fig. 2). A positive dispersion as large as 10% was in that case observed. The evaluation of the positive dispersion effect at high pressure is more difficult since, to the best of our knowledge, ultrasound measurements are limited to only two data sets: one extending to 0.06 GPa and 1500 K (Ref. 20) and the other to 0.7 GPa and 423 K.[21] We can use the value at 0.3 GPa and 423 K (Ref. 21) to compare with our data set at the same pressure and 493 K [see Fig. 2(b)] as the temperature dependence of the ultrasound velocity at that pressure is found to be negligible.[21] This comparison suggests the existence at 0.3 GPa of a positive dispersion up to about 8%, in qualitative agreement with the room pressure result.

In Fig. 2(b) we report as well, for the 3.2 GPa pressure value, the sound velocity as derived, in the infinite-frequency elastic limit, from the following expression:[1]

$$v_L(q) = \sqrt{\frac{3k_BT}{M} + \frac{n}{Mq^2}\int \frac{\partial^2 V}{\partial z^2}(1-e^{-iqz})g(r)d^3r}, \quad (1)$$

where we have used the pair-correlation function $g(r)$ obtained by us in the previously referred to diffraction experiment. In this calculation, we refer to the Price potential V, which is an empty core pseudopotential with the Coulomb ion-ion repulsion screened by the valence electrons.[11] As for the dielectric screening function we use the one proposed by Singwi *et al.*,[22] successfully used also in the simulation of liquid alkali metals at the melting point.[10] This model of potential relies on three parameters: the ion core radius which marks the extension of the empty core region, the effective mass, and the density of the valence electrons, which affect the electronic screening. Following Price *et*

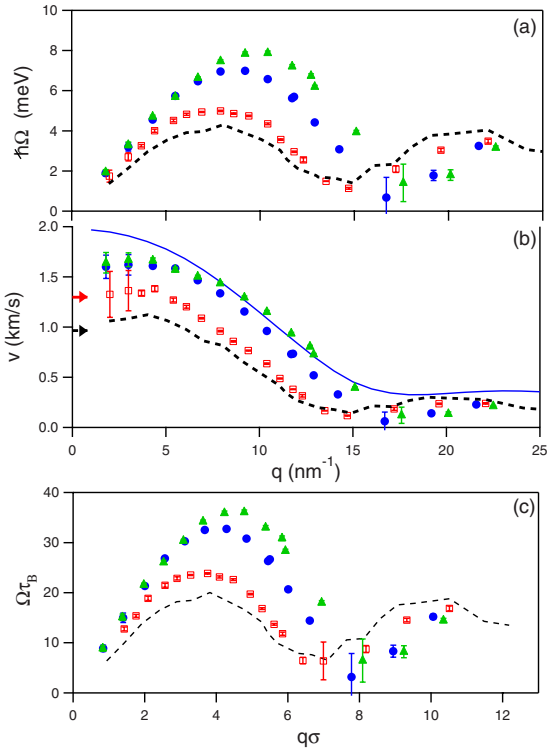

FIG. 2. (Color online) (a) Dispersion curve and (b) phase velocity of the acoustic excitations at 0.3 (□), 3.2 (●), and 5 GPa (▲). Dashed lines: neutron-scattering results at the room pressure melting point (Ref. 3). Full line in panel (b): infinite-frequency elastic sound velocity at 3.2 GPa calculated using Eq. (1). Horizontal arrows in panel (b): ultrasound velocities at the room pressure melting point (lower arrow) and at 0.3 GPa and 423 K (upper arrow) (Refs. 20 and 21). The same dispersion curves are reported in reduced units in panel (c) following Ref. 10.

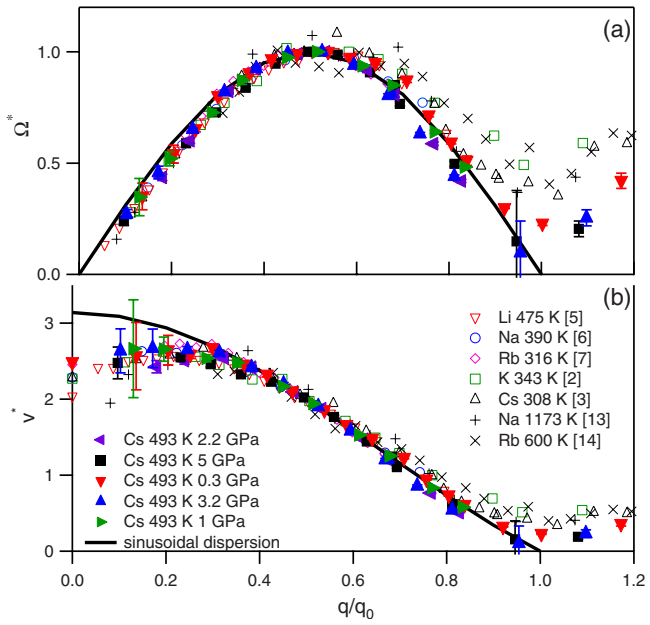

FIG. 3. (Color online) (a) Scaled dispersion curves and (b) sound velocity data from the present work together with literature results [see legend in panel (b)]. The $q=0$ values are the corresponding adiabatic sound velocities (Refs. 19 and 21). The solid line corresponds to a simple sinusoidal dispersion curve.

al.,[11] Balucani *et al.*,[9,10] and Mountain[23] we consider the first two parameters as constant so that pressure affects the potential only via its explicit density dependence. From Fig. 2(b) it is clear that the apparent sound velocity and that in the elastic limit do not match, though they are close in a q range around the maximum of the dispersion curve: the high-frequency regime for the acoustic excitations probed by inelastic x-ray or neutron scattering does not correpond to the infinite-frequency elastic limit. This observation confirms previous results, e.g., those of a numerical simulation study of liquid Cs at room pressure and temperature[1] and has been usually discussed invoking the presence of additional relaxation channels.[1]

The dispersion curves that we measured allow us to test over a large density range the scaling scheme originally proposed by Balucani *et al.*[10] for liquid metals at their melting point. For this purpose, we derive from the calculated potential the parameters σ and ϵ corresponding to the investigated densities and use them to scale our experimental data, as reported in Fig. 2(c) for the dispersion curves of Fig. 2(a): it is clear that they do not collapse on a single curve. Since σ is nearly density independent (the modifications induced by pressure concern mainly the attractive part of the potential), this implies that the density dependence of ϵ is not able to account for that of the acoustic frequencies. Nevertheless, the similarity of the dispersion curves reported here encourages us to further investigate the possible existence of a scaling law. In fact, we find a universal behavior of the acoustic dispersion for $0.15q_0 \leq q \leq 0.7q_0$ if we use the reduced units $q^*=q/q_0$ and $\Omega^*=\Omega/\Omega_0$, Ω_0 being the maximum of the dispersion curve (see Fig. 3). Furthermore, this same scaling procedure nicely works also for all the data available for liquid alkali metals, both at melting[2–7] and at high temperature.[12–14] We can then conclude that all the measured acoustic dispersion curves of liquid alkali metals share the same shape: it is enough to provide q_0 and Ω_0 to fix them completely. In other words, temperature- and density-dependent relaxation processes are only relevant at low q where the positive dispersion of the sound velocity becomes visible. In this macroscopic range, in fact, the scaling law is lost as the $q=0$ limit of the acoustic velocity, i.e., the adiabatic velocity, does not simply scale with the high-frequency one, as shown in Fig. 3(b). The scaling fails as well at high q, with $q>0.7q_0$, where the free particle limit is approached. In this regime, indeed, the dispersion curves are mainly affected by the atomic mass and by the thermodynamic conditions. It is interesting to note as well that the universal curve found here closely resembles at high q^* the sinusoidal dispersion expected in the case of a harmonic crystal with nearest-neighbor interactions (solid line in Fig. 3). The deviations from it are mostly localized in the low q range ($q^* \leq 0.3$), as highlighted in Fig. 3(b), where the scaled sound velocity is reported.

The results reported in Fig. 3 suggest that a unique effective pair potential can be used for liquid alkali metals also at very different thermodynamic conditions. To test this point, we have calculated $qv_L(q)$ from Eq. (1) using the Price potential as discussed above together with literature data for the

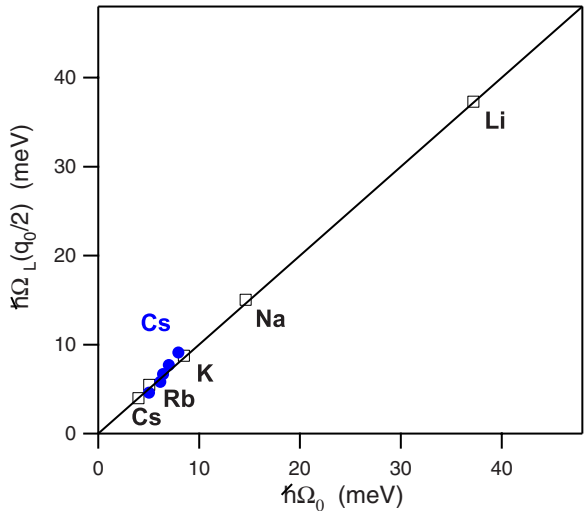

FIG. 4. (Color online) Theoretical (y-axis) vs experimental (x-axis) values of the acoustic frequency at the maximum of the dispersion curve ($q=q_0/2$). Squares: data at the melting point; bullets: high-pressure Cs.

$g(r)$ of all the alkali metals at the melting point[24] and the $g(r)$ obtained by us for high-pressure Cs. As previously said, the experimental frequencies do not correspond to the infinite frequency elastic limit; still the dispersion curves are very close to the prediction of Eq. (1) at the position of their maximum, $q=q_0/2$. In Fig. 4 we thus compare the results of this calculation at $q=q_0/2$ with the measured Ω_0. A convincing correspondence is found between theoretical estimations and experimental data; this shows the ability of the potential we have used to successfully describe the high-frequency dynamics of liquid alkali metals over a large density range. A closer inspection of Fig. 4 shows deviations for Cs up to 15% over a density range that, however, changes by a factor of 2. This might be due to a difference increasing with density between the measured dispersion curve and the corresponding elastic prediction or, more likely, to the inaccuracy at very high density of our simplified treatment of the density dependence of the potential. It is worth noticing that Mountain[23] reported that this same potential was not able to reproduce the intensity of the first peak of the static structure factor of liquid Rb at high temperature. However, in the q region concerned here, i.e., $0.15 \leq q^* \leq 0.7$, the theoretical and experimental structure factors were found to agree within a few percent; in this q range, then, the Price potential is able to well reproduce both the structural and the dynamical properties of liquid alkali metals. Finally, we want to remark that no special changes take place at the liquid-liquid transition in Cs which is mainly of electronic character and where the electronic screening might be expected to change significantly.

Summing up, the study of the high-frequency dynamics of liquid Cs at high density has allowed us to investigate the relation between dynamical properties of liquid alkali metals and the details of the pair potential. We have identified a universal scaling of the acoustic dispersion curve which holds for very different packing fractions and electronic screening contributions. This has two main consequences: (i) the high-frequency acoustic dynamics of liquid alkali metals is basically unaffected by temperature- and density-dependent relaxation processes at least for $q \geq 0.15 q_0$, and (ii) a unique model of interatomic potential is able to describe these systems for densities changing by as much as a factor of 2. The pseudopotential formulated by Price *et al.*[11] is shown here to be a good approximation for it, even if only its explicit density dependence is taken into account. Further improvement could be achieved by considering the pressure-induced changes in the bare ion-ion interaction and in the valence electron contribution.

We are grateful to H. Müller and M. Hanfland for their help in the sample preparation and in the diffraction experiment and to C. Henriquet for technical assistance.

[1] U. Balucani and M. Zoppi, *Dynamics of the Liquid State* (Clarendon, Oxford, 1994).
[2] J. R. D. Copley and J. M. Rowe, Phys. Rev. Lett. **32**, 49 (1974).
[3] T. Bodensteiner *et al.*, Phys. Rev. A **45**, 5709 (1992).
[4] L. E. Bove *et al.*, Phys. Rev. B **68**, 024208 (2003).
[5] T. Scopigno *et al.*, Phys. Rev. Lett. **85**, 4076 (2000).
[6] T. Scopigno *et al.*, Phys. Rev. E **65**, 031205 (2002).
[7] A. Monaco *et al.*, J. Chem. Phys. **120**, 8089 (2004).
[8] W. C. Pilgrim and C. Morkel, J. Phys.: Condens. Matter **18**, R585 (2006).
[9] U. Balucani *et al.*, Phys. Rev. A **46**, 2159 (1992).
[10] U. Balucani *et al.*, Phys. Rev. B **47**, 3011 (1993).
[11] D. L. Price *et al.*, Phys. Rev. B **2**, 2983 (1970).
[12] T. Scopigno *et al.*, J. Phys.: Condens. Matter **12**, 8009 (2000).
[13] W. C. Pilgrim *et al.*, J. Non-Cryst. Solids **250**-252, 96 (1999).
[14] F. Demmel *et al.*, Phys. Rev. B **74**, 184207 (2006).
[15] S. Falconi *et al.*, Phys. Rev. Lett. **94**, 125507 (2005).
[16] S. Falconi and G. J. Ackland, Phys. Rev. B **73**, 184204 (2006).
[17] www.esrf.fr/UsersAndScience/Experiments/HRRS/ID16
[18] R. S. Hixson and J. N. Fritz, J. Appl. Phys. **71**, 1721 (1992).
[19] T. Scopigno *et al.*, Rev. Mod. Phys. **77**, 881 (2005).
[20] N. B. Vargaftik *et al.*, Int. J. Thermophys. **7**, 821 (1986).
[21] G. H. Shaw and D. A. Caldwell, Phys. Rev. B **32**, 7937 (1985).
[22] K. S. Singwi *et al.*, Phys. Rev. B **1**, 1044 (1970).
[23] R. D. Mountain, J. Phys. F: Met. Phys. **8**, 1637 (1978).
[24] Y. Waseda, *The Structure of Non-Crystalline Materials* (McGraw-Hill, New York, 1980).